

Bayesian physical reconstruction of initial conditions from large-scale structure surveys

paper by Jens Jasche & Benjamin D. Wandelt

Lorenzo Cavezza - 2130648

12/02/25

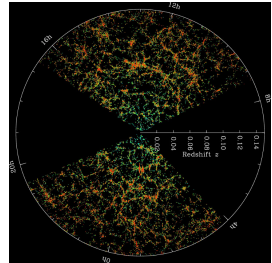
Table of contents

1. Introduction
2. Bayesian Framework
3. HMC
4. Testing
5. Conclusions

Introduction

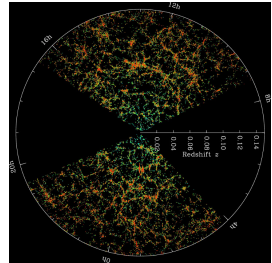
Standard Approach

- Tracers' Surveys (Galaxy Surveys)



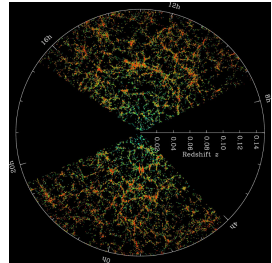
Standard Approach

- Tracers' Surveys (Galaxy Surveys)
- Initial Conditions Constraining



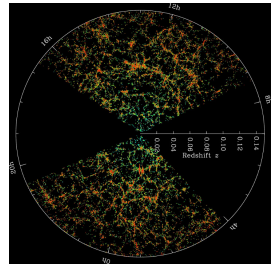
Standard Approach

- Tracers' Surveys (Galaxy Surveys)
- Initial Conditions Constraining
- Evolved Density Field Approximations



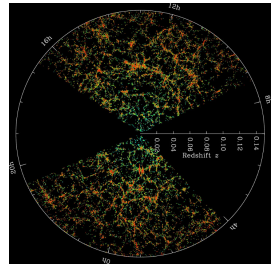
Standard Approach

- Tracers' Surveys (Galaxy Surveys)
- Initial Conditions Constraining
- Evolved Density Field Approximations



Standard Approach

- Tracers' Surveys (Galaxy Surveys)
- Initial Conditions Constraining
- Evolved Density Field Approximations



Proposed Alternative

- 2LPT dynamically evolved final density field prior
- Hamiltonian Monte Carlo exploration of initial field conditioned on mock observations

Bayesian Framework

The non - Gaussian Prior

Given a model of **LSS** formation $G(a, \delta^i)$ (a *Second Order Lagrangian Perturbation Theory* model (**2LPT**) in our case), we obtain the final density contrast δ^f prior as:

$$\mathcal{P}(\{\delta_l^f\}) = \int d\{\delta_l^i\} \mathcal{P}(\{\delta_l^i\}, \{\delta_l^f\} \mid \mathbf{s}) =$$

The non - Gaussian Prior

Given a model of **LSS** formation $G(a, \delta^i)$ (a *Second Order Lagrangian Perturbation Theory* model (**2LPT**) in our case), we obtain the final density contrast δ^f prior as:

$$\begin{aligned}\mathcal{P}(\{\delta_l^f\}) &= \int d\{\delta_l^i\} \mathcal{P}(\{\delta_l^i\}, \{\delta_l^f\} \mid \mathbf{s}) = \\ &= \int d\{\delta_l^i\} \mathcal{P}(\{\delta_l^f\} \mid \{\delta_l^i\}) \mathcal{P}(\{\delta_l^i\} \mid \mathbf{s}) =\end{aligned}$$

The non - Gaussian Prior

Given a model of **LSS** formation $G(a, \delta^i)$ (a *Second Order Lagrangian Perturbation Theory* model (**2LPT**) in our case), we obtain the final density contrast δ^f prior as:

$$\begin{aligned}\mathcal{P}(\{\delta_l^f\}) &= \int d\{\delta_l^i\} \mathcal{P}(\{\delta_l^i\}, \{\delta_l^f\} \mid \mathbf{s}) = \\ &= \int d\{\delta_l^i\} \mathcal{P}(\{\delta_l^f\} \mid \{\delta_l^i\}) \mathcal{P}(\{\delta_l^i\} \mid \mathbf{s}) = \\ &= \int d\{\delta_l^i\} \prod_l \delta^D(\delta_l^f - G(a, \delta^i)_l) \left(\frac{e^{-\frac{1}{2} \sum_{lm} \delta_l^i \mathbf{s}_{lm}^{-1} \delta_m^i}}{\det(2\pi \mathbf{S})} \right)\end{aligned}$$

The non - Gaussian Prior

Given a model of **LSS** formation $G(a, \delta^i)$ (a *Second Order Lagrangian Perturbation Theory* model (**2LPT**) in our case), we obtain the final density contrast δ^f prior as:

$$\begin{aligned}\mathcal{P}(\{\delta_l^f\}) &= \int d\{\delta_l^i\} \mathcal{P}(\{\delta_l^i\}, \{\delta_l^f\} \mid \mathbf{S}) = \\ &= \int d\{\delta_l^i\} \mathcal{P}(\{\delta_l^f\} \mid \{\delta_l^i\}) \mathcal{P}(\{\delta_l^i\} \mid \mathbf{S}) = \\ &= \int d\{\delta_l^i\} \prod_l \delta^D(\delta_l^f - G(a, \delta^i)_l) \left(\frac{e^{-\frac{1}{2} \sum_{lm} \delta_l^i \mathbf{S}_{lm}^{-1} \delta_m^i}}{\det(2\pi \mathbf{S})} \right)\end{aligned}$$

with \mathbf{S} representing the initial contrast covariance matrix.

This can be done through sampling of $\mathcal{P}(\{\delta_l^f\}, \{\delta_l^i\} \mid \mathbf{S})$ and discarding the δ_l^i realization

The LSS Likelihood

We can model the observed tracers, namely galaxies, through an *inhomogeneous Poisson Likelihood*:

$$\mathcal{P} \left(\{N_k^g\} \mid \{\lambda_k\} \right) = \prod_k \frac{(\lambda_k)^{N_k^g} e^{-\lambda_k}}{N_k^g!}$$

The LSS Likelihood

We can model the observed tracers, namely galaxies, through an *inhomogeneous Poisson Likelihood*:

$$\mathcal{P} \left(\{N_k^g\} \mid \{\lambda_k\} \right) = \prod_k \frac{(\lambda_k)^{N_k^g} e^{-\lambda_k}}{N_k^g!}$$

with

- N_k^g : observed galaxy number at position x_k
- λ_k : expected galaxy number at x_k :

$$\lambda_k = \lambda_k(\delta) = R_k \bar{N} (1 + B(\delta^f)_k)$$

The LSS Likelihood

We can model the observed tracers, namely galaxies, through an *inhomogeneous Poisson Likelihood*:

$$\mathcal{P} \left(\{N_k^g\} \mid \{\lambda_k\} \right) = \prod_k \frac{(\lambda_k)^{N_k^g} e^{-\lambda_k}}{N_k^g!}$$

with

- N_k^g : observed galaxy number at position x_k
- λ_k : expected galaxy number at x_k :

$$\lambda_k = \lambda_k(\delta) = R_k \bar{N} (1 + B(\delta^f)_k)$$

where:

- R_k : survey geometries and selection functions linear operator
- $B(x)_k$: non linear and non local bias operator

The 2LPT - Poisson Posterior

The joint posterior of the final and initial contrast densities is:

$$\mathcal{P}\left(\{\delta_l^f\}, \{\delta_l^i\} \mid \{N_i\}, \mathbf{S}\right) =$$

The 2LPT - Poisson Posterior

The joint posterior of the final and initial contrast densities is:

$$\begin{aligned} \mathcal{P} \left(\{ \delta_l^f \}, \{ \delta_l^i \} \mid \{ N_i \}, \mathbf{S} \right) = \\ = \prod_k \frac{(\lambda_k(\delta^f))^{N_k^g} e^{-\lambda_k(\delta^f)}}{N_k^g!} \prod_l \delta^D \left(\delta_l^f - G(a, \delta^i)_l \right) \left(\frac{e^{-\frac{1}{2} \sum_{lm} \delta_l^i \mathbf{S}_{lm}^{-1} \delta_m^i}}{\det(2\pi \mathbf{S})} \right) \end{aligned}$$

The 2LPT - Poisson Posterior

The joint posterior of the final and initial contrast densities is:

$$\begin{aligned} \mathcal{P} \left(\{ \delta_l^f \}, \{ \delta_l^i \} \mid \{ N_i \}, \mathbf{S} \right) = \\ = \prod_k \frac{(\lambda_k(\delta^f))^{N_k^g} e^{-\lambda_k(\delta^f)}}{N_k^g!} \prod_l \delta^D \left(\delta_l^f - G(a, \delta^i)_l \right) \left(\frac{e^{-\frac{1}{2} \sum_{lm} \delta_l^i \mathbf{S}_{lm}^{-1} \delta_m^i}}{\det(2\pi \mathbf{S})} \right) \end{aligned}$$

which leads to the marginalized initial density posterior:

$$\mathcal{P} \left(\{ \delta_l^i \} \mid \{ N_i \}, \mathbf{S} \right) = \prod_k \frac{(\lambda_k(G(a, \delta^i)))^{N_k^g} e^{-\lambda_k(G(a, \delta^i))}}{N_k^g!} \left(\frac{e^{-\frac{1}{2} \sum_{lm} \delta_l^i \mathbf{S}_{lm}^{-1} \delta_m^i}}{\det(2\pi \mathbf{S})} \right)$$

The 2LPT - Poisson Posterior

The joint posterior of the final and initial contrast densities is:

$$\mathcal{P} \left(\{ \delta_l^f \}, \{ \delta_l^i \} \mid \{ N_i \}, \mathbf{S} \right) = \\ = \prod_k \frac{(\lambda_k(\delta^f))^{N_k^g} e^{-\lambda_k(\delta^f)}}{N_k^g!} \prod_l \delta^D \left(\delta_l^f - G(a, \delta^i)_l \right) \left(\frac{e^{-\frac{1}{2} \sum_{lm} \delta_l^i \mathbf{S}_{lm}^{-1} \delta_m^i}}{\det(2\pi \mathbf{S})} \right)$$

which leads to the marginalized initial density posterior:

$$\mathcal{P} \left(\{ \delta_l^i \} \mid \{ N_i \}, \mathbf{S} \right) = \prod_k \frac{(\lambda_k(G(a, \delta^i)))^{N_k^g} e^{-\lambda_k(G(a, \delta^i))}}{N_k^g!} \left(\frac{e^{-\frac{1}{2} \sum_{lm} \delta_l^i \mathbf{S}_{lm}^{-1} \delta_m^i}}{\det(2\pi \mathbf{S})} \right)$$

Benefits:

- Forward Model Evaluation
- All uncertainties accounted (survey geometry, selection biases, galaxy distribution noise and cosmic variance)

Hamiltonian Monte Carlo

- Why *HMC*?

- Why *HMC*?

$\Rightarrow 2 \cdot 10^6$ parameters to infer (box's voxels) \Rightarrow very low acceptance
in random walk based MC (*curse of dimensionality*)

- Why *HMC*?

- ⇒ $2 \cdot 10^6$ parameters to infer (box's voxels) ⇒ very low acceptance in random walk based MC (*curse of dimensionality*)
- ⇒ *HMC* yields an acceptance of nearly 1 (integration errors)

- Why *HMC*?

⇒ $2 \cdot 10^6$ parameters to infer (box's voxels) ⇒ very low acceptance in random walk based MC (*curse of dimensionality*)

⇒ *HMC* yields an acceptance of nearly 1 (integration errors)

- *HMC* moves smoothly inside *typical volumes* by exploiting well defined equations of motion through the *Hamiltonian*:

$$H = \sum_i \sum_j \frac{1}{2} p_i \mathbf{M}_{ij}^{-1} p_j + \psi(x) = \sum_i \sum_j \frac{1}{2} p_i \mathbf{M}_{ij}^{-1} p_j - \ln \mathcal{P}(x)$$

- Why *HMC*?

⇒ $2 \cdot 10^6$ parameters to infer (box's voxels) ⇒ very low acceptance in random walk based MC (*curse of dimensionality*)

⇒ *HMC* yields an acceptance of nearly 1 (integration errors)

- *HMC* moves smoothly inside *typical volumes* by exploiting well defined equations of motion through the *Hamiltonian*:

$$H = \sum_i \sum_j \frac{1}{2} p_i \mathbf{M}_{ij}^{-1} p_j + \psi(x) = \sum_i \sum_j \frac{1}{2} p_i \mathbf{M}_{ij}^{-1} p_j - \ln \mathcal{P}(x)$$

$$\Rightarrow e^{-H} = \mathcal{P}(\{x_i\}) \exp \left(-\frac{1}{2} \sum_i \sum_j p_i \mathbf{M}_{ij}^{-1} p_j \right)$$

- Why *HMC*?

⇒ $2 \cdot 10^6$ parameters to infer (box's voxels) ⇒ very low acceptance in random walk based MC (*curse of dimensionality*)

⇒ *HMC* yields an acceptance of nearly 1 (integration errors)

- *HMC* moves smoothly inside *typical volumes* by exploiting well defined equations of motion through the *Hamiltonian*:

$$H = \sum_i \sum_j \frac{1}{2} p_i \mathbf{M}_{ij}^{-1} p_j + \psi(x) = \sum_i \sum_j \frac{1}{2} p_i \mathbf{M}_{ij}^{-1} p_j - \ln \mathcal{P}(x)$$

$$\Rightarrow e^{-H} = \mathcal{P}(\{x_i\}) \exp \left(-\frac{1}{2} \sum_i \sum_j p_i \mathbf{M}_{ij}^{-1} p_j \right)$$

- Momenta randomly drawn and easily marginalized as nuisance parameters. After dynamical evolution the *acceptance probability* is

$$\mathcal{P}_A = \min [1, \exp (-(H(\{x'_i\}, \{p'_i\}) - H(\{x_i\}, \{p_i\})))]$$

LSS Equations of Motion

We get the Equations of Motion through *Hamilton's equations*:

LSS Equations of Motion

We get the Equations of Motion through *Hamilton's equations*:

$$\frac{d\delta_n^i}{dt} = \frac{\partial H}{\partial p_i} = \sum_j \mathbf{M}_{nj}^{-1} p_j \quad \text{with} \quad \mathbf{M}_{nj} = \mathbf{S}_{nj}^{-1} - \delta_{nj}^K D^1 \left. \frac{\partial \mathbf{J}_j(s)}{\partial s_j} \right|_{s_j=\xi_j}$$

LSS Equations of Motion

We get the Equations of Motion through *Hamilton's equations*:

$$\frac{d\delta_n^i}{dt} = \frac{\partial H}{\partial p_i} = \sum_j \mathbf{M}_{nj}^{-1} p_j \quad \text{with} \quad \mathbf{M}_{nj} = \mathbf{S}_{nj}^{-1} - \delta_{nj}^K D^1 \left. \frac{\partial \mathbf{J}_j(s)}{\partial s_j} \right|_{s_j=\xi_j}$$

The Hamiltonian mass optimizes the integrator's stability . Vector \mathbf{J} accounts for the gradient of the first order approximate "Zeldovich" potential.

LSS Equations of Motion

We get the Equations of Motion through *Hamilton's equations*:

$$\frac{d\delta_n^i}{dt} = \frac{\partial H}{\partial p_i} = \sum_j \mathbf{M}_{nj}^{-1} p_j \quad \text{with} \quad \mathbf{M}_{nj} = \mathbf{S}_{nj}^{-1} - \delta_{nj}^K D^1 \left. \frac{\partial \mathbf{J}_j(s)}{\partial s_j} \right|_{s_j=\xi_j}$$

The Hamiltonian mass optimizes the integrator's stability . Vector \mathbf{J} accounts for the gradient of the first order approximate "Zeldovich" potential. We define the potential of the Hamiltonian system explicitly:

$$\Psi(\{\delta_l^i\}) = -\ln\left(\mathcal{P}\left(\{\delta_l^i\} \mid \{N_i\}, \mathbf{S}\right)\right)$$

LSS Equations of Motion

We get the Equations of Motion through *Hamilton's equations*:

$$\frac{d\delta_n^i}{dt} = \frac{\partial H}{\partial p_i} = \sum_j \mathbf{M}_{nj}^{-1} p_j \quad \text{with} \quad \mathbf{M}_{nj} = \mathbf{S}_{nj}^{-1} - \delta_{nj}^K D^1 \left. \frac{\partial \mathbf{J}_j(s)}{\partial s_j} \right|_{s_j=\xi_j}$$

The Hamiltonian mass optimizes the integrator's stability . Vector \mathbf{J} accounts for the gradient of the first order approximate "Zeldovich" potential. We define the potential of the Hamiltonian system explicitly:

$$\Psi(\{\delta_l^i\}) = -\ln(\mathcal{P}(\{\delta_l^i \mid \{N_i\}, \mathbf{S}\})) = \Psi_{prior}(\{\delta_l^i\}) + \Psi_{likelihood}(\{\delta_l^i\}) =$$

LSS Equations of Motion

We get the Equations of Motion through *Hamilton's equations*:

$$\frac{d\delta_n^i}{dt} = \frac{\partial H}{\partial p_i} = \sum_j \mathbf{M}_{nj}^{-1} p_j \quad \text{with} \quad \mathbf{M}_{nj} = \mathbf{S}_{nj}^{-1} - \delta_{nj}^K D^1 \left. \frac{\partial \mathbf{J}_j(s)}{\partial s_j} \right|_{s_j=\xi_j}$$

The Hamiltonian mass optimizes the integrator's stability . Vector \mathbf{J} accounts for the gradient of the first order approximate "Zeldovich" potential. We define the potential of the Hamiltonian system explicitly:

$$\begin{aligned} \Psi(\{\delta_l^i\}) &= -\ln(\mathcal{P}(\{\delta_l^i \mid \{N_i\}, \mathbf{S}\})) = \Psi_{prior}(\{\delta_l^i\}) + \Psi_{likelihood}(\{\delta_l^i\}) = \\ &= \frac{1}{2} \sum_{lm} \delta_l^i \mathbf{S}_{lm}^{-1} \delta_m^i + \sum_k [R_k \bar{N} (1 + G(a, \delta^i)_k) - N_k \ln(R_k \bar{N} (1 + G(a, \delta^i)_k))] \end{aligned}$$

LSS Equations of Motion

We get the Equations of Motion through *Hamilton's equations*:

$$\frac{d\delta_n^i}{dt} = \frac{\partial H}{\partial p_i} = \sum_j \mathbf{M}_{nj}^{-1} p_j \quad \text{with} \quad \mathbf{M}_{nj} = \mathbf{S}_{nj}^{-1} - \delta_{nj}^K D^1 \left. \frac{\partial \mathbf{J}_j(s)}{\partial s_j} \right|_{s_j=\xi_j}$$

The Hamiltonian mass optimizes the integrator's stability . Vector \mathbf{J} accounts for the gradient of the first order approximate "Zeldovich" potential. We define the potential of the Hamiltonian system explicitly:

$$\begin{aligned} \Psi(\{\delta_l^i\}) &= -\ln(\mathcal{P}(\{\delta_l^i \mid \{N_i\}, \mathbf{S}\})) = \Psi_{prior}(\{\delta_l^i\}) + \Psi_{likelihood}(\{\delta_l^i\}) = \\ &= \frac{1}{2} \sum_{lm} \delta_l^i \mathbf{S}_{lm}^{-1} \delta_m^i + \sum_k [R_k \bar{N} (1 + G(a, \delta^i)_k) - N_k \ln(R_k \bar{N} (1 + G(a, \delta^i)_k))] \\ &\implies \frac{dp_n^i}{dt} = -\frac{\partial \Psi_{prior}(\{\delta_l^i\})}{\partial \delta_p^i} - \frac{\partial \Psi_{likelihood}(\{\delta_l^i\})}{\partial \delta_p^i} = \end{aligned}$$

LSS Equations of Motion

We get the Equations of Motion through *Hamilton's equations*:

$$\frac{d\delta_n^i}{dt} = \frac{\partial H}{\partial p_i} = \sum_j \mathbf{M}_{nj}^{-1} p_j \quad \text{with} \quad \mathbf{M}_{nj} = \mathbf{S}_{nj}^{-1} - \delta_{nj}^K D^1 \left. \frac{\partial \mathbf{J}_j(s)}{\partial s_j} \right|_{s_j=\xi_j}$$

The Hamiltonian mass optimizes the integrator's stability . Vector \mathbf{J} accounts for the gradient of the first order approximate "*Zeldovich*" potential. We define the potential of the Hamiltonian system explicitly:

$$\begin{aligned} \Psi(\{\delta_l^i\}) &= -\ln(\mathcal{P}(\{\delta_l^i \mid \{N_i\}, \mathbf{S}\})) = \Psi_{prior}(\{\delta_l^i\}) + \Psi_{likelihood}(\{\delta_l^i\}) = \\ &= \frac{1}{2} \sum_{lm} \delta_l^i \mathbf{S}_{lm}^{-1} \delta_m^i + \sum_k [R_k \bar{N} (1 + G(a, \delta^i)_k) - N_k \ln(R_k \bar{N} (1 + G(a, \delta^i)_k))] \\ &\implies \frac{dp_n^i}{dt} = -\frac{\partial \Psi_{prior}(\{\delta_l^i\})}{\partial \delta_p^i} - \frac{\partial \Psi_{likelihood}(\{\delta_l^i\})}{\partial \delta_p^i} = \\ &= -\sum_j \mathbf{S}_{pj}^{-1} \delta_j^i + D^1 J_n - D^2 \sum_{a>b} (\tau_n^{aabb} - \tau_n^{bbaa} - 2\tau_n^{abab}) \end{aligned}$$

where the τ_m^{abcd} accounts for the gradient of the second order lagrangian potential.

The Leapfrog Method

As an integration scheme the Leapfrog Method is used:

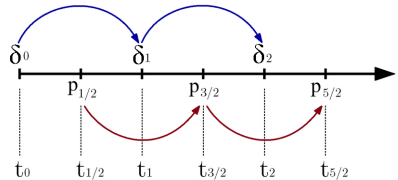
⇒ simplest integration method that conserves the energy and phase space area and is time reversible

The Leapfrog Method

As an integration scheme the Leapfrog Method is used:

⇒ simplest integration method that conserves the energy and phase space area and is time reversible

$$\begin{aligned}p_m(t + \frac{\epsilon}{2}) &= p_m(t) - \frac{\epsilon}{2} \frac{\partial \psi(\{\delta_k^i\})}{\delta_f^i} \bigg|_{\delta_m^i(t)} \\ \delta_m^i(t + \epsilon) &= \delta_m^i(t) - \frac{\epsilon}{m_i} p_m(t + \frac{\epsilon}{2}) \\ p_m(t + \epsilon) &= p_m(t + \frac{\epsilon}{2}) - \frac{\epsilon}{2} \frac{\partial \psi(\{\delta_k^i\})}{\delta_f^i} \bigg|_{\delta_m^i(t+\epsilon)}\end{aligned}$$

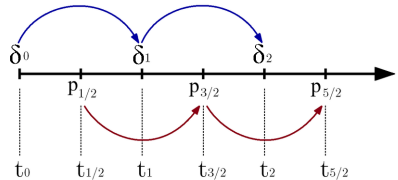


The Leapfrog Method

As an integration scheme the Leapfrog Method is used:

⇒ simplest integration method that conserves the energy and phase space area and is time reversible

$$\begin{aligned} p_m(t + \frac{\epsilon}{2}) &= p_m(t) - \frac{\epsilon}{2} \frac{\partial \psi(\{\delta_k^i\})}{\delta_j^i} \bigg|_{\delta_m^i(t)} \\ \delta_m^i(t + \epsilon) &= \delta_m^i(t) - \frac{\epsilon}{m_i} p_m(t + \frac{\epsilon}{2}) \\ p_m(t + \epsilon) &= p_m(t + \frac{\epsilon}{2}) - \frac{\epsilon}{2} \frac{\partial \psi(\{\delta_k^i\})}{\delta_j^i} \bigg|_{\delta_m^i(t+\epsilon)} \end{aligned}$$



which translates to:

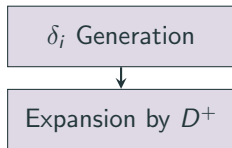
$$\begin{aligned} p_m(t + \epsilon) &= p_m(t) - \frac{\epsilon}{2} \left(\frac{\partial \Psi(\delta^i)}{\partial \delta_j^i} \bigg|_{\delta^i(t)} + \frac{\partial \Psi(\delta^i)}{\partial \delta_m^i} \bigg|_{\delta^i(t+\epsilon)} \right) \\ \delta_m(t + \epsilon) &= \delta_m(t) + \epsilon \sum_j M_{mj}^{-1} p_j(t) - \frac{\epsilon^2}{2} \sum_j M_{mj}^{-1} \frac{\partial \Psi(\delta^i)}{\partial \delta_j^i} \bigg|_{\delta^i(t)} \end{aligned}$$

Testing the Model

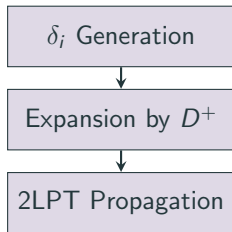
Mock Observations

δ_i Generation

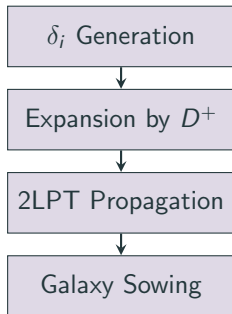
Mock Observations



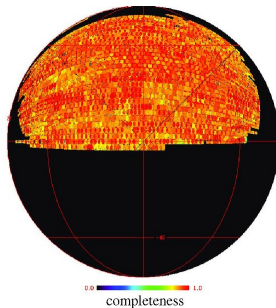
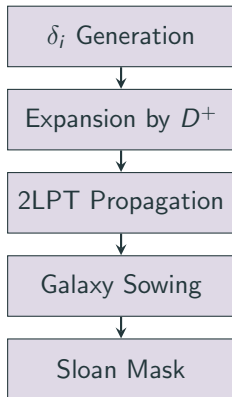
Mock Observations



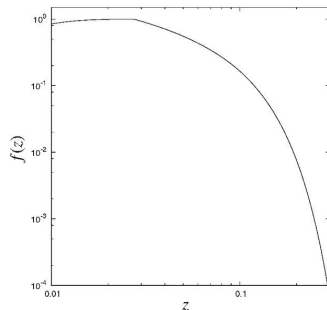
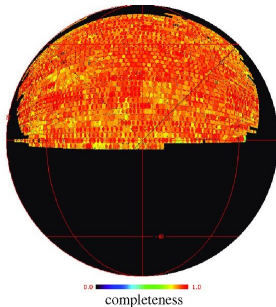
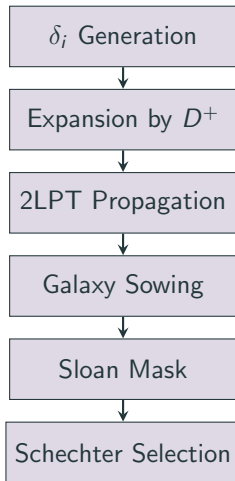
Mock Observations



Mock Observations



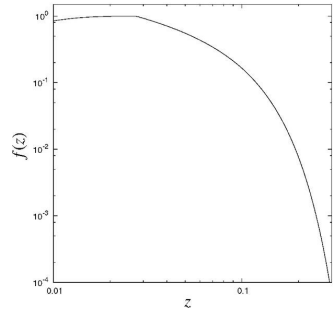
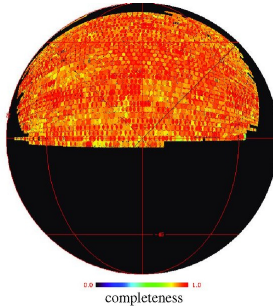
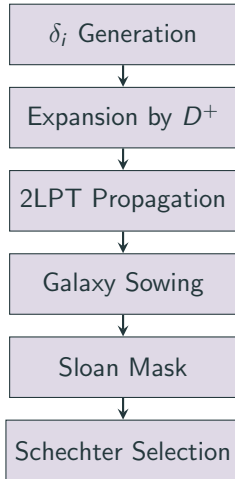
Mock Observations



$$\text{with: } f(z) = \frac{\int_{M_{\min}^{\max}(z)}^{M_{\max}} \Phi(M) dM}{\int_{M_{\min}}^{M_{\max}} \Phi(M) dM}$$

where $\Phi(M)$ is the *Schechter* luminosity function.

Mock Observations



$$\text{with: } f(z) = \frac{\int_{M_{\min}}^{M_{\max}(z)} \Phi(M) dM}{\int_{M_{\min}}^{M_{\max}} \Phi(M) dM}$$

where $\Phi(M)$ is the *Schechter* luminosity function.
The linear operator used in Poisson Sampling is:

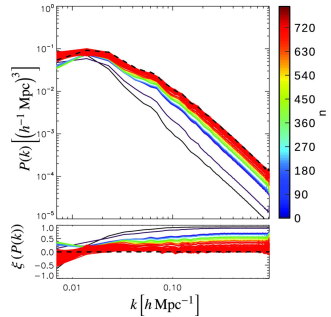
$$R_i = M_i F_i = M(\alpha_i, \delta_i) f^l(z_i)$$

- Arbitrarily lower strength δ_l^i by one tenfold
- Quantify power spectra drift with:

$$\xi(P_i(K)) = 1 - \frac{P_i(k)}{P^0(k)}$$

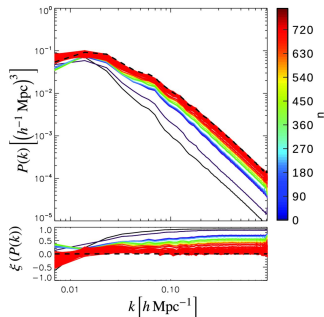
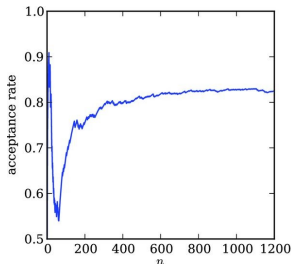
- Arbitrarily lower strength δ_l^i by one tenfold
- Quantify power spectra drift with:

$$\xi(P_i(K)) = 1 - \frac{P_i(k)}{P^0(k)}$$



- Arbitrarily lower strength δ_i^j by one tenfold
- Quantify power spectra drift with:

$$\xi(P_i(K)) = 1 - \frac{P_i(k)}{P^0(k)}$$



- Acceptance takes a dip after manual drift
- Back to normal ($\sim 84\%$) after ~ 600 epochs

Autocorrelation is computed to determine the number of independent samples and to assess good mixing:

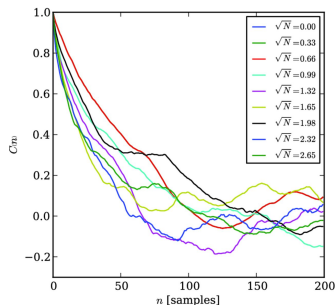
$$C(\delta)_n = \left\langle \frac{\delta^i - \langle \delta \rangle}{\sqrt{\text{Var}(\delta)}} \frac{\delta^{i+n} - \langle \delta \rangle}{\sqrt{\text{Var}(\delta)}} \right\rangle$$

Autocorrelation

Autocorrelation is computed to determine the number of independent samples and to assess good mixing:

$$C(\delta)_n = \left\langle \frac{\delta^i - \langle \delta \rangle}{\sqrt{\text{Var}(\delta)}} \frac{\delta^{i+n} - \langle \delta \rangle}{\sqrt{\text{Var}(\delta)}} \right\rangle$$

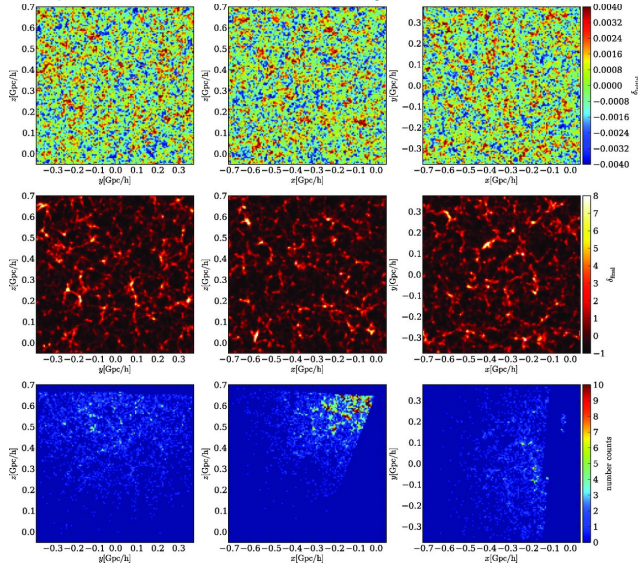
We see such correlations plotted from different signal-to-noise ratios \sqrt{N}



$C(\delta)_n < 0.1$ when $n \sim 200 \implies$ correlation length is about 200

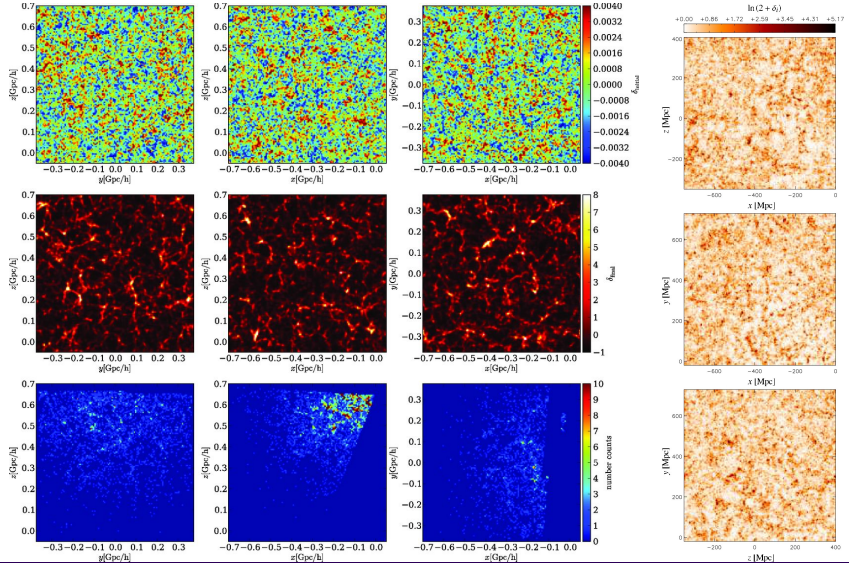
Inferred Density Fields

Samples from the sampled density fields and mock data:



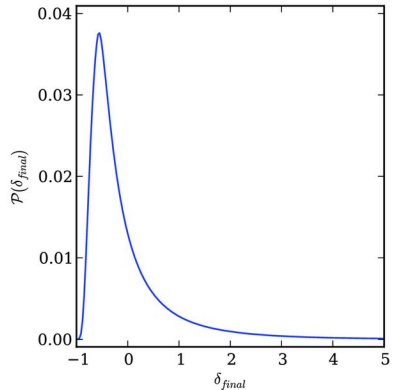
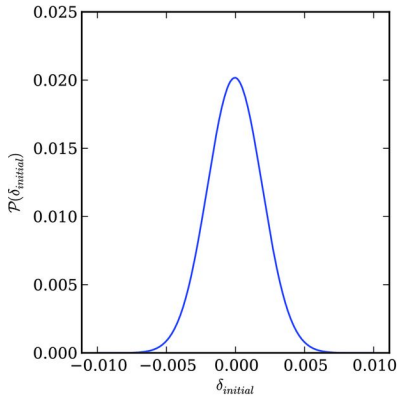
Inferred Density Fields

Samples from the sampled density fields and mock data:



Inferred Density Fields

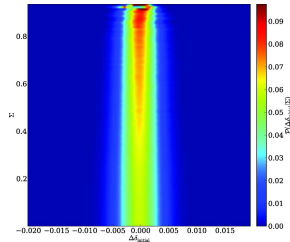
One-point distribution of density contrasts:



Accuracy

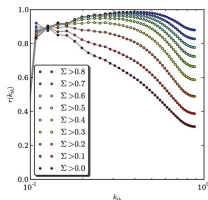
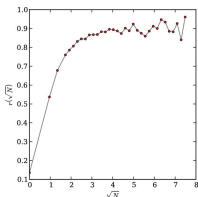
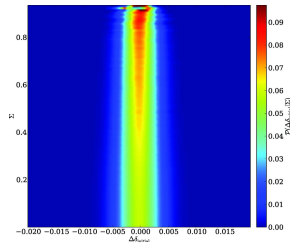
Inferred initial density accuracy is assessed with the posterior of $\Delta\delta_{initial} = \delta_{initial}^{true} - \delta_{initial}$ conditioned to a signal-to-noise ratio proxy:

$$\Sigma = \frac{|\langle\delta_{initial}\rangle|}{\sqrt{\langle(\delta_{initial} - \langle\delta_{initial}\rangle)^2\rangle}}$$



Inferred initial density accuracy is assessed with the posterior of $\Delta\delta_{initial} = \delta_{initial}^{true} - \delta_{initial}$ conditioned to a signal-to-noise ratio proxy:

$$\Sigma = \frac{|\langle\delta_{initial}\rangle|}{\sqrt{\langle(\delta_{initial} - \langle\delta_{initial}\rangle)^2\rangle}}$$

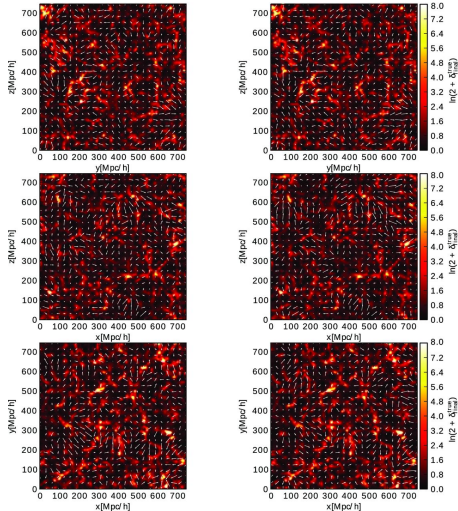


The correlation coefficient between inferred and real densities is computed as a function of \sqrt{N} for the final and of k for different Σ for the initial:

$$r(k_x) = \frac{\langle\delta_0^x \langle\delta\rangle^x\rangle}{\sqrt{\langle(\delta_0^x)^2\rangle}\sqrt{\langle(\delta^x)^2\rangle}}$$

Inferred Dynamics

True vs inferred dynamics:



Conclusions

Conclusions

- Successfully implemented a forward propagation Bayesian dynamical LSS inference algorithm that correctly accounts for high order statistics in generating initial and final density fields through HMC and 2LPT conditioning on mock data

Conclusions

- Successfully implemented a forward propagation Bayesian dynamical LSS inference algorithm that correctly accounts for high order statistics in generating initial and final density fields through HMC and 2LPT conditioning on mock data
- Achieved low correlation length, short burn - in phase and good mixing, as well as impressive reconstruction capabilities in masked regions

Conclusions

- Successfully implemented a forward propagation Bayesian dynamical LSS inference algorithm that correctly accounts for high order statistics in generating initial and final density fields through HMC and 2LPT conditioning on mock data
- Achieved low correlation length, short burn - in phase and good mixing, as well as impressive reconstruction capabilities in masked regions
- High accuracy in final and initial inferred fields, in particular for high signal-to-noise regions and large scales

Conclusions

- Successfully implemented a forward propagation Bayesian dynamical LSS inference algorithm that correctly accounts for high order statistics in generating initial and final density fields through HMC and 2LPT conditioning on mock data
- Achieved low correlation length, short burn - in phase and good mixing, as well as impressive reconstruction capabilities in masked regions
- High accuracy in final and initial inferred fields, in particular for high signal-to-noise regions and large scales
- Faithful reconstruction of the final density velocity field

Conclusions

- Successfully implemented a forward propagation Bayesian dynamical LSS inference algorithm that correctly accounts for high order statistics in generating initial and final density fields through HMC and 2LPT conditioning on mock data
- Achieved low correlation length, short burn - in phase and good mixing, as well as impressive reconstruction capabilities in masked regions
- High accuracy in final and initial inferred fields, in particular for high signal-to-noise regions and large scales
- Faithful reconstruction of the final density velocity field
- Possible further improvements include better model errors and accuracy of 2LPT, real galaxy surveys tests, and incorporation of halo-mode-based galaxy bias models

Thank you for your attention
